Bootstrap inversion for P_n wave velocity in North-Western Italy

Stefano Parolai, Daniele Spallarossa and Claudio Eva
Dipartimento di Scienze della Terra, Sezione di Geofisica, Università di Genova, Italy

Abstract
An inversion of P_n arrival times from regional distance earthquakes (180-800 km), recorded by 94 seismic stations operating in North-Western Italy and surrounding areas, was carried out to image lateral variations of *P*-wave velocity at the crust-mantle boundary, and to estimate the static delay time at each station. The reliability of the obtained results was assessed using both synthetic tests and the bootstrap Monte Carlo resampling technique. Numerical simulations demonstrated the existence of a trade-off between cell velocities and estimated station delay times along the edge of the model. Bootstrap inversions were carried out to determine the standard deviation of velocities and time terms. Low P_n velocity anomalies are detected beneath the outer side of the Alps (−6%) and the Western Po plain (−4%) in correspondence with two regions of strong crustal thickening and negative Bouguer anomaly. In contrast, high P_n velocities are imaged beneath the inner side of the Alps (+4%) indicating the presence of high velocity and density lower crust-upper mantle. The Ligurian sea shows high P_n velocities close to the Ligurian coastlines (+3%) and low P_n velocities (−1.5%) in the middle of the basin in agreement with the upper mantle velocity structure revealed by seismic refraction profiles.

Key words *P_n wave – tomography – bootstrap – Italy*

1. Introduction

The present day structural setting of North-Western Italy results from several tectonic events driven by the relative movements between Eurasia and Africa plates (Dewey *et al.*, 1989). In particular, the late Cretaceous collision between Adria and European plates formed the Alpine chain and determined the rise of a slice of heavy mantle (Ivrea body) up to the shallower crustal layers (Polino *et al.*, 1990); the convergence process was accomplished by a strong deepening of the European Moho down to a maximum of 50-60 km. The opening of the Ligurian-Provençal basin (Rehault *et al.*, 1984), related to the eastward migrations of the Corsican-Sardinian block, and the orogenesis of the Apennines, caused the thinning of the crust in the Ligurian sea and the formation of a crustal indenting between the Ligurian lithosphere and the North-Western Apennines (fig. 1) (Buness *et al.*, 1990; Laubscher *et al.*, 1992).

In recent decades much effort has been spent collecting reliable information on the three dimensional structure of the lithosphere system; strong crustal heterogeneities have already been detected mainly from refraction (DSS profiles and EGT project) and reflection (ECORS-CROP; Swiss NFP-20) studies carried out from 1967 to the present day.

The great number of studies carried out in this area supplied mainly local information: Kissling (1993) was able to compile a whole 3D image of the litho-asthenosphere system

Mailing address: Dr. Stefano Parolai, Dipartimento di Scienze della Terra, Sezione di Geofisica, Università di Genova, Viale Benedetto XV, 5, 16132 Genova, Italy; e-mail: stefano2@dister.unige.it

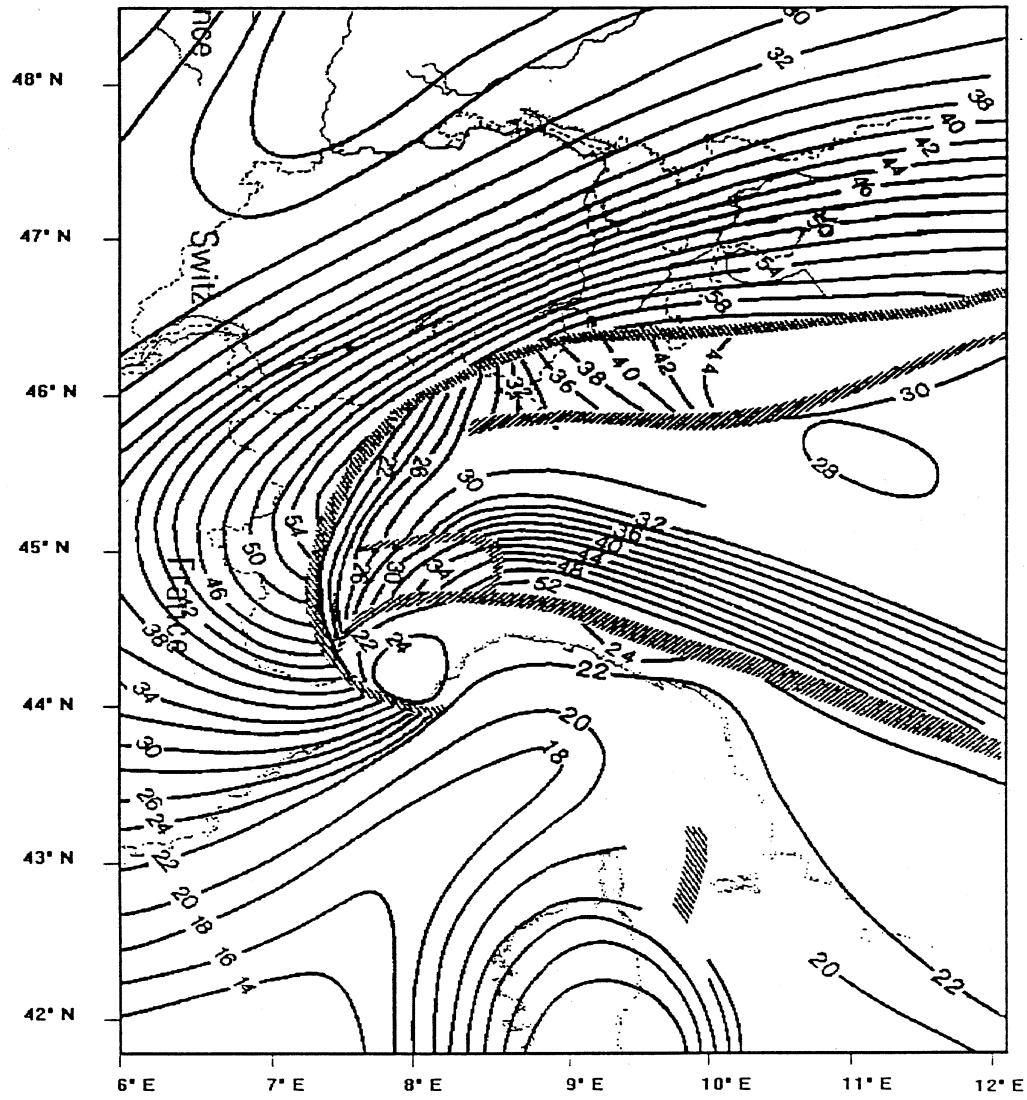

Fig. 1. A Moho map of North-Western Italy (Giese and Buness, 1992).

beneath the Alpine chain by comparing results of different geophysical studies (refraction and reflection profiles, seismic tomography); however their non-homogeneous geographic distribution, and their variable reliability do not allow an unambiguous interpretation. While the depth of the European and the Adria Moho beneath the Alps has been reliably mapped by many studies, the crustal thickness under the Po plain and the geometrical relationships between Adria and the Ligurian Moho are still poorly understood.

As the regional phases travel nearly horizontally in the upper mantle, they are particularly predisposed to detect the lateral heterogeneities of the lithosphere.

In a previous paper, Parolai *et al.* (1997) outlined the presence of strong lateral velocity variations at the crustal mantle boundary using the inversion of a P_n arrivals data set.

The present paper is mainly devoted to an analysis of the reliability of inversion results in an area showing strong lateral velocity contrasts. The final results were tested with numerical simulations using different test models and the confidence interval of the solution was evaluated by the bootstrap method. Moreover, to image the P_n propagation anomalies a more complete data set, with respect to Parolai *et al.* (1997), was inverted.

2. Data

Travel time arrival picks recorded from 1982 to 1995 by the IGG (Genova), EOPG (Strasburg), SISMALP (Grenoble), ETH (Zurich) and ING (Rome) networks were used in this study.

The investigated area was laterally extended considering data coming from different seismic networks.

As shown in fig. 2,, the station distribution represents a geometrically non-homogeneous network because stations are mainly installed to monitor the most seismically active areas of the Alps and Apennines.

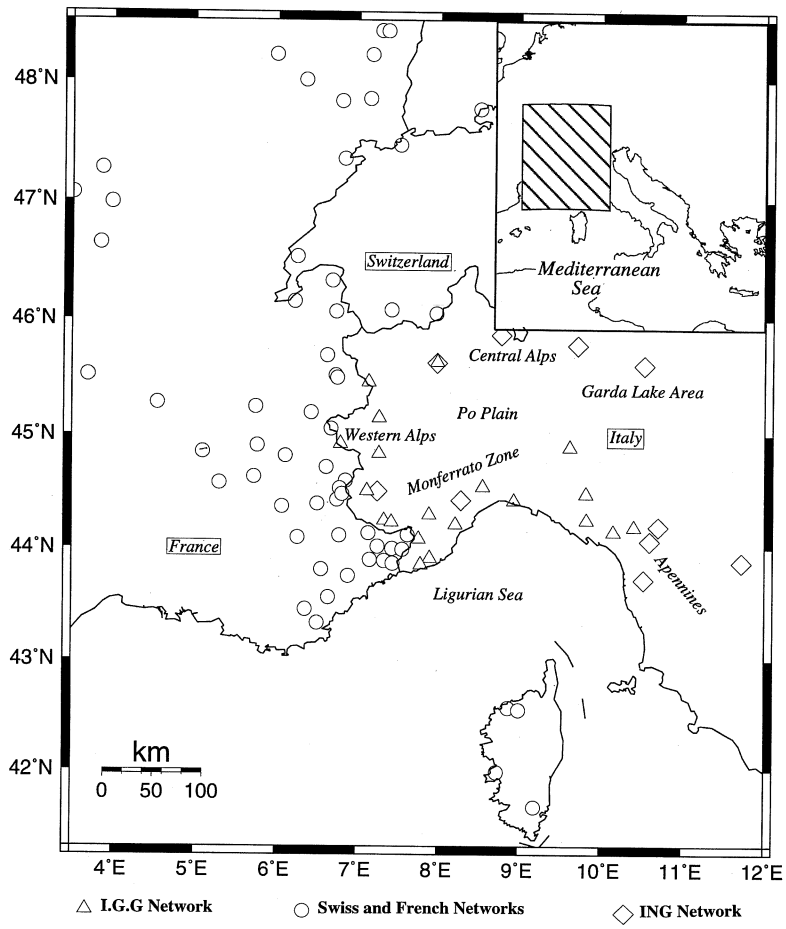

Fig. 2. Distribution of the stations used in this study. Symbols indicate different networks.

The large number of Bulletin data collected was then submitted to a selection procedure that can be summarized as follow:

– the events with an azimuthal gap too wide to guarantee a stable hypocentral location were eliminated;

– each earthquake was relocated considering all the recording stations at distance < 300 km;

– following the suggestion of Hearn *et al.* (1991), the data were windowed to compute the mean crustal slowness, the mean crustal delay, and the mean Moho depth, using an iterative procedure that results in a least squares straight line to fit the data. A mean depth of the Moho of 30 km, a mean Moho velocity of 8 km/s and a mean crustal velocity of 6.2 km/s were calculated and adopted as a starting model;

– to obtain a high quality P_n data set a further careful selection was performed considering: 1) only first arrivals recorded at a distance greater than 180 km; 2) only stations with a number of readings greater than 10; 3) only earthquakes recorded by at least five stations at distance greater than 180 km; 4) travel times with maximum residuals of 1.5 s with respect to the travel times computed from the starting model including a correction both for the station elevations and the depths of the events.

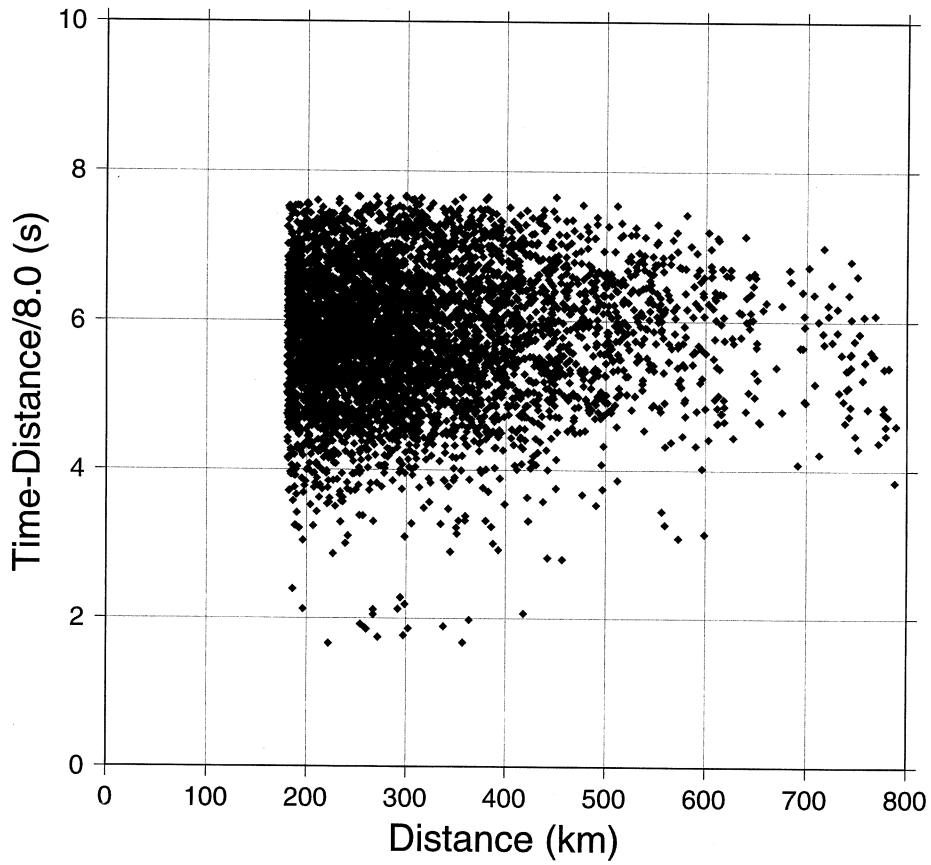

Fig. 3. Travel time plot of selected phases recorded from 1982 to 1995.

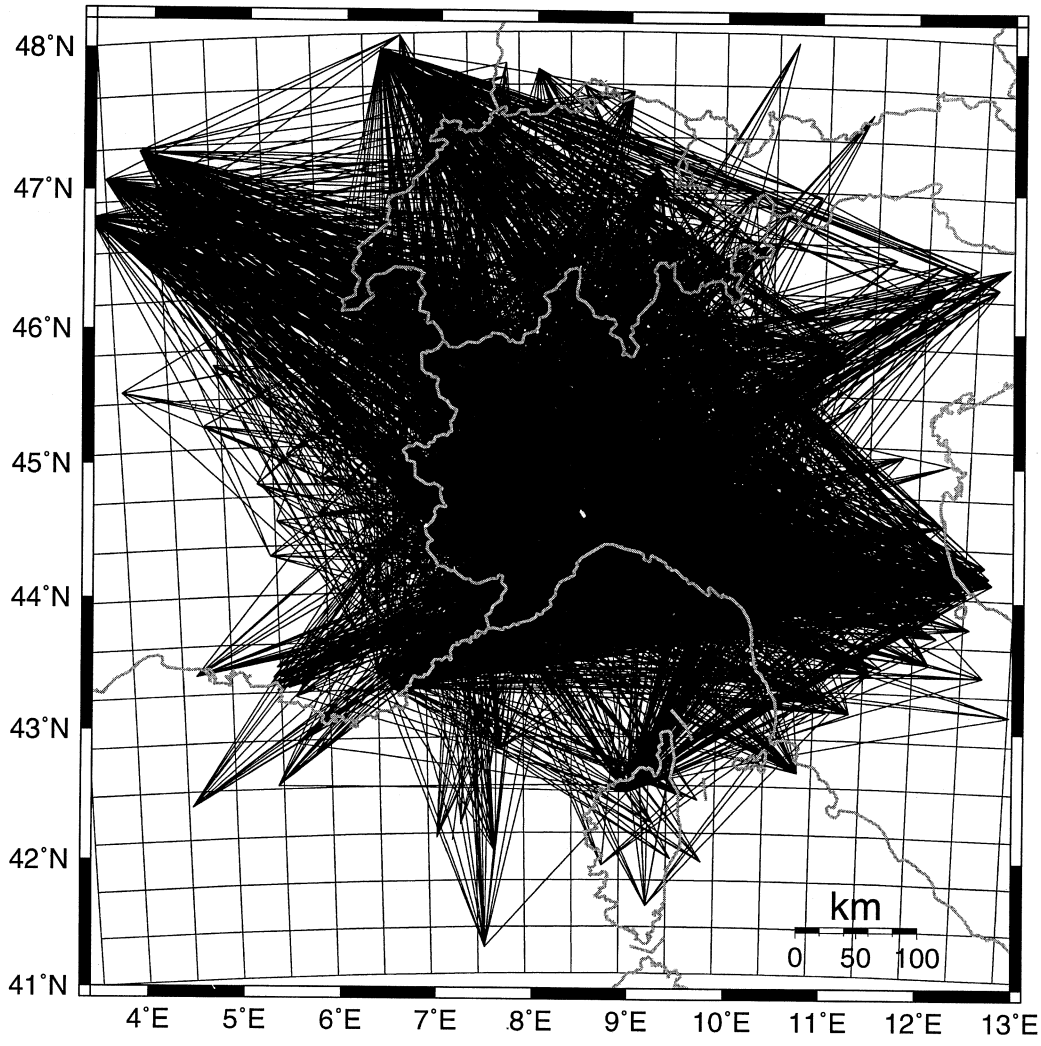

Fig. 4. Cell parametrization used in this study (40 km×40 km) and selected ray paths.

A total of 5400 rays from 400 events were screened out of the original data set of almost 25000 arrivals (fig. 3). In fig. 4 the distribution of the selected 5400 ray paths is reported. Even if the event distribution seems to be quite homogeneous, the station distribution makes the ray path coverage satisfactory only in the center of the model where also a high number of crossing rays per cell exists.

3. Method

Detailed description of the method is given in Hearn (1984); here we will briefly review it.

Refracted ray paths can be described as the sum of three portions: the source-to-mantle ray path, the ray path through the mantle, and the ray path from the mantle to the receiver.

Therefore the travel times for these P_n ray paths can be described by the time term equation (Willmore and Bancroft, 1960; Hearn, 1984) as:

$$t = a+b+Ds \tag{3.1}$$

where a and b are the delay times for stations and events respectively, D is the source receiver distance and s is the mantle slowness.

Delay times are expressed in terms of crustal thickness and crustal velocity:

$$\text{delay} = \int (s_c^2 - s^2)^{1/2} \, dz \tag{3.2}$$

where s_c is the crustal slowness profile as a function of depth.

As pointed out by many authors in previous works (Hearn, 1984; Hearn and Clayton, 1986; Grand, 1990), station delays depend on crustal and mantle velocities and crustal thickness while event delays also take into account errors in source depth, origin time determination and systematic picking errors at the station. Moreover, as station delays are sensitive more to crustal thickness variations than to mantle velocity changes (Braile *et al.*, 1989) they are mainly interpreted in terms of Moho depth (Hearn *et al.*, 1991).

Using a data set composed of many event-station pairs and parametrizing the mantle velocity field into a 2D grid of cells, the entire set of time term equations (3.1) may be written as:

$$\boldsymbol{A}\boldsymbol{x} = \boldsymbol{t} \tag{3.3}$$

where the vector $\boldsymbol{x}$ contains the unknown time terms and the unknown slowness perturbation, $\boldsymbol{t}$ is a vector of the observed P_n travel time residuals. The matrix $\boldsymbol{A}$ contains mostly zeros; namely each row contains two elements equal to 1 corresponding to the station and the event, and the elements representing the distance the current ray travels in each cell.

In order to obtain the solution of the linear equation system (3.3) a preconditioned version of the LSQR algorithm (Paige and Saunders, 1982) was used.

Moreover, to implement the regularization properties of the adopted iterative method, a set of equations, that requires the Laplacian difference of the model to vanish, was also included.

Weighting the regularization equations with a control parameter λ, it is also possible to control the trade-off between the travel time fitting and the roughness of the model: the constraint on the Laplacian limits only the total amount of slowness fluctuation, not the individual slowness contrasts (Lees and Crosson, 1989). More detailed description of the adopted inversion is given in Hearn and Ni (1994).

In order to image the velocity anomalies, the investigated area was divided into square cells measuring 40×40 km. The travel time data set was inverted using a reference model which considers a mean crustal velocity of 6.2 km/s, a mean crustal thickness of 30 km, and a P_n velocity of 8.0 km/s.

4. Reliability test and bootstrap analysis

One of the main problems commonly encountered in every tomographic study is the determination of the reliability of the results: tomographic images reflect not only true velocity heterogeneities but also the effect of data errors, model parametrization, ray path geometry and algorithm performance (Spakman and Nolet, 1988).

In recent years, numerical simulations have become increasingly popular to assess the resolution power both of the inversion method and of the data set (among others Evans and Achauer, 1993; Alessandrini *et al.*, 1995; Solarino *et al.*, 1996).

Numerical simulation with synthetics allows the verification of the capability of ray path geometry to solve anomalous patterns by measuring the similarity between the final model and the arbitrary model used to compute the synthetics.

Leveque *et al.* (1993) have shown that using this approach may lead to wrong conclusions. They demonstrate that, in contrast with a generally accepted idea, although an inversion scheme can accurately retrieve small-size structures, it is not necessarily able to retrieve larger structures.

Since the choice of the parametrization of the model biases the tomographic results, they suggest either resorting to a suitable but unfortunately computationally very demanding inversion procedure or to assess the resolution for different test models.

On this basis, following previous P_n studies (Hearn and Ni, 1994), sensitivity tests were carried out using two different test models: the first model consisting of a checkerboard velocity pattern having a square shape with 40 km sides, whereas the second one was composed of four large regions, having alternatively velocity perturbations of ±6% (fig. 5), each one constituted by 90 square cells with sides of 40 km.

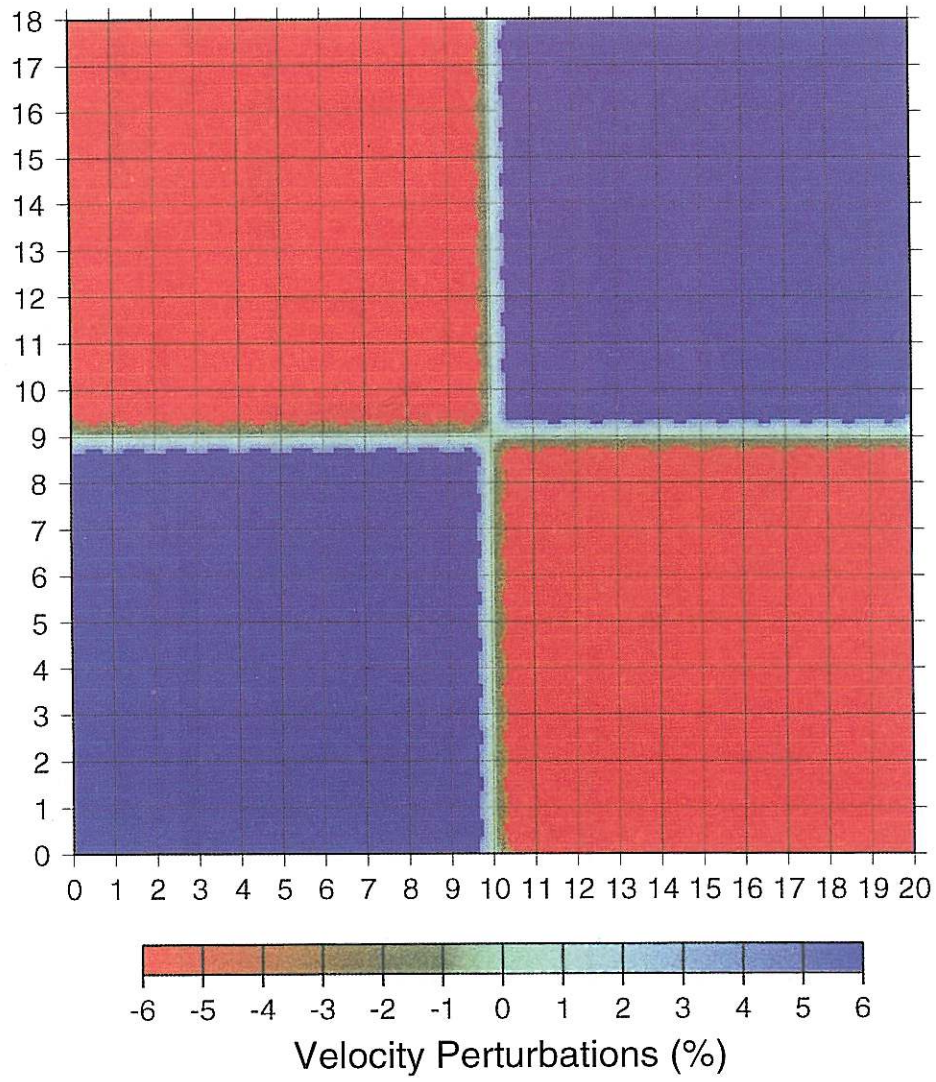

Fig. 5. Sketch of the second model used for synthetic tests.

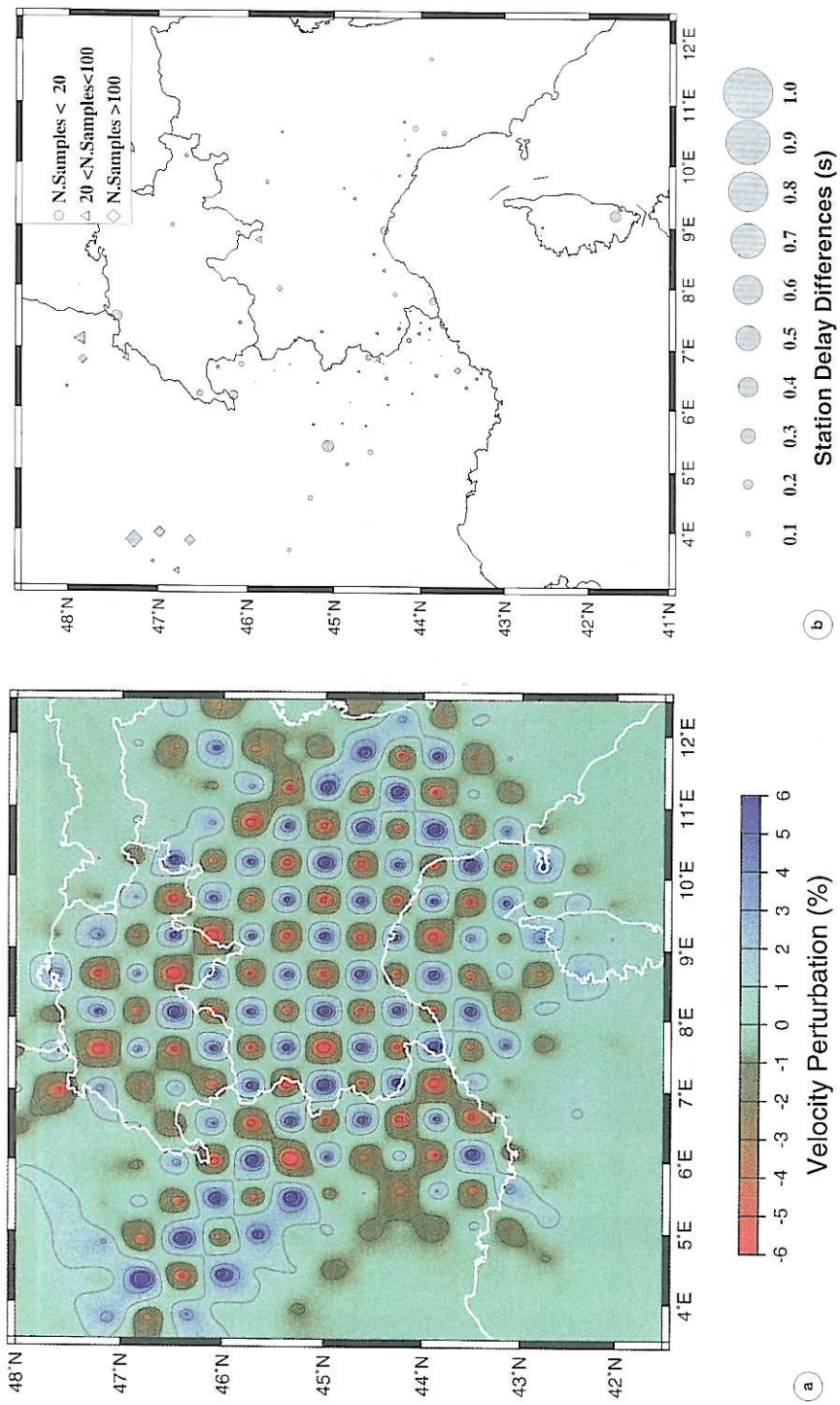

Fig. 6a,b. Result of the inversion of synthetic data generated with the checkerboard test model: a) output model; b) differences between input and computed station delay times. The symbol shape depends on the number of samples for each station, while the dimension is proportional to the size of the station delay error.

In addition zero-mean normally distributed random noise with standard deviation corresponding to the r.m.s. of the observed residuals was included. Random values ranging from 1 s to 4 s were also assigned to the synthetic delays. Finally, aiming at overcoming the inherent limitations of the sensitivity test analysis and avoiding possible misinterpretations of the tomographic image, the confidence intervals of the results were estimated using a bootstrap resampling technique.

Figure 6a,b shows the results of the syntetic inversion obtained through the first test model (checkerboard): in the central part of the investigated area the original checkerboard pattern appears quite well retrieved (fig. 6a) due to the complete azimuthal ray path coverage, whereas at the edge of the model the effects generated by scarce ray paths and lack of crossing rays are evident. In general, as the adopted backprojection inversion method smoothes over large velocity adjustment in the poorly sampled cells, marginal zones show mainly low values of perturbations. Moreover, in some areas such as Eastern Switzerland and North-Eastern Italy, because of strongly inhomogeneous ray path coverage, the anomalies are extended in ray direction.

Figure 6b reports test results for the station delay times: large errors, relevant only for stations placed along the edges of the model, do not seem to depend on the number of arrivals.

The checkerboard test can be useful in identifying the well-solved areas of the model. Nevertheless, especially when a small grid size parametrization has been adopted, it cannot satisfactorily point out whether there is a trade-off between station delays and the mantle velocity field (Hearn and Ni, 1994); consequently, some tests were carried out using the second model.

Looking at the test results for the second model (fig. 7a,b), and comparing them with the previous ones obtained using the checkerboard pattern, the different behaviour between inner and outer stations is clearly shown: while both tests show small error (< 0.3 s) for the former, the results of the latter test display large errors (doubled with respect to the ones obtained by the checkerboard test) affecting the stations at the edges. Some peripheral French stations (fig. 7b), previously carefully solved (fig. 6b), show errors greater than 0.8 s. Therefore we can state that, along the edge of the model, the trade-off between station delays and mantle velocity cannot be fully resolved.

With respect to the velocity perturbations (fig. 7a), the best resolution in terms of retrieving the original anomaly distribution is, again, observed only in the central part of the model where the boundaries between the four large regions appear well reproduced.

Bootstrap methods (Efron, 1979; Koch, 1992; Hearn and Ni, 1994) are being increasingly used with the advent of more powerful computers. These techniques work by repeated inversions of the bootstrap data sets obtained by randomly resampling, with replacement, the original data set. We used a number of 1000 bootstrap inversion iterations to obtain a good estimate of the standard deviation of the solution.

The results of the bootstrap inversion are shown in fig. 8 and fig. 9a,b. The standard deviation for the velocity cells of the tomographic model (fig. 8) range from 0.09 km/s to 0.24 km/s. The highest errors appear at the edge of the image where a lack of crossing rays exists, whereas the Alps and the Po plain show standard deviation values of about of 0.1 km/s: the latter value, assuming a mean Moho velocity of 8.0 km/s, is equivalent to a velocity perturbation of 1.2%, well below the size of the velocity anomalies found inverting the whole data set (see fig. 10). The average standard deviation for station delays (fig. 9a,b) is lower than 0.2 s but, in this case, higher errors are more related to the number of rays per station than to the marginal position within the investigated area.

As shown in fig. 9b, the standard deviation monotonically decreases with the increasing number of sampling rays. This behaviour could explain why, in some cases, neighbouring stations (Ligurian coast) show an error difference greater than 0.3 s. Nevertheless, poorly sampled stations (fig. 9b), with fewer than 20 rays, show strong differences in estimated errors that could be related to scarce ray path coverage affecting marginal stations.

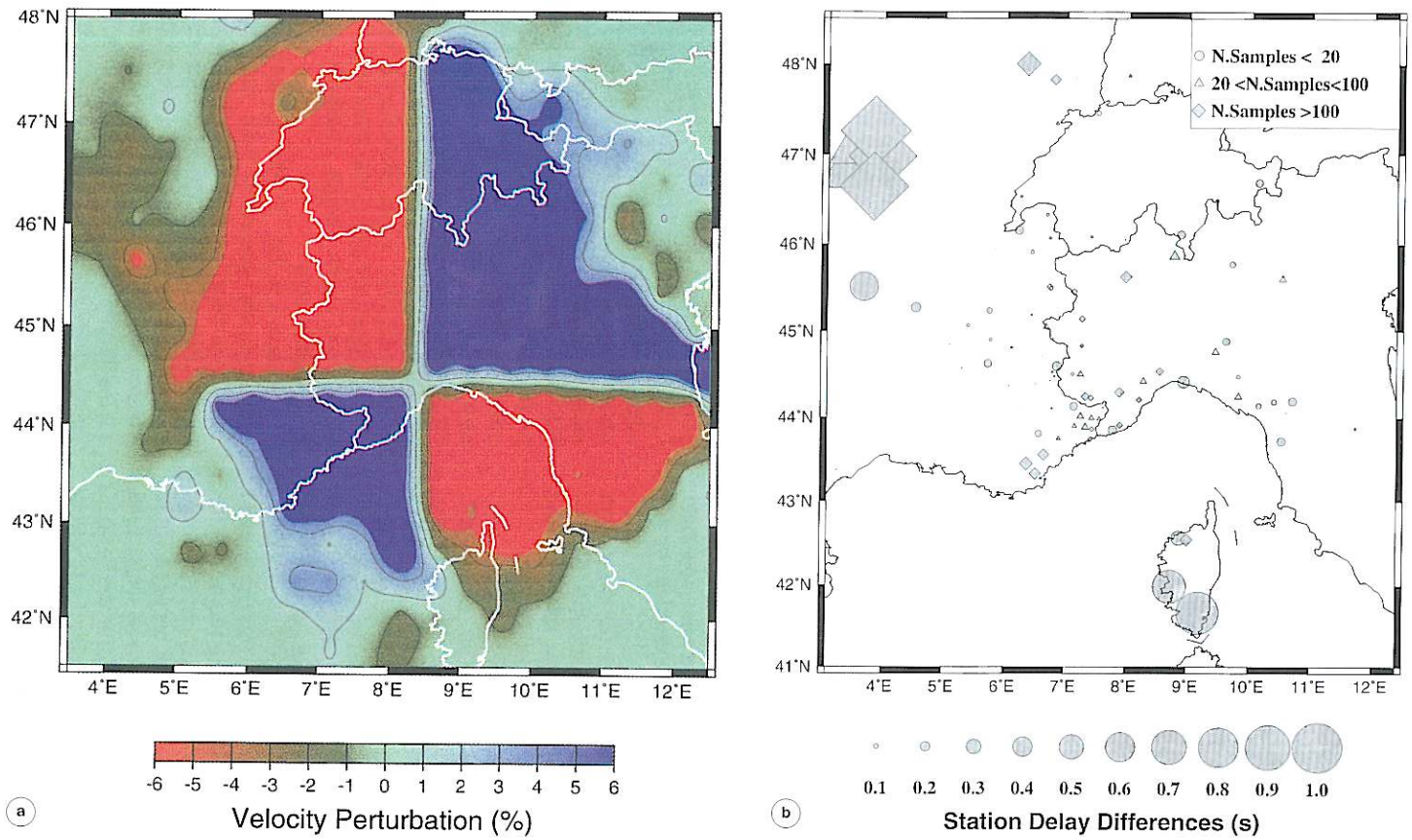

Fig. 7a,b. Result of the inversion of synthetic data generated with the second test model composed of only four anomalous regions each one constituted by 90 cells: a) output model; b) differences between input and computed station delay times. The symbol shape depends on the number of sample for each station, while the dimension is proportional to the size of the station delay error.

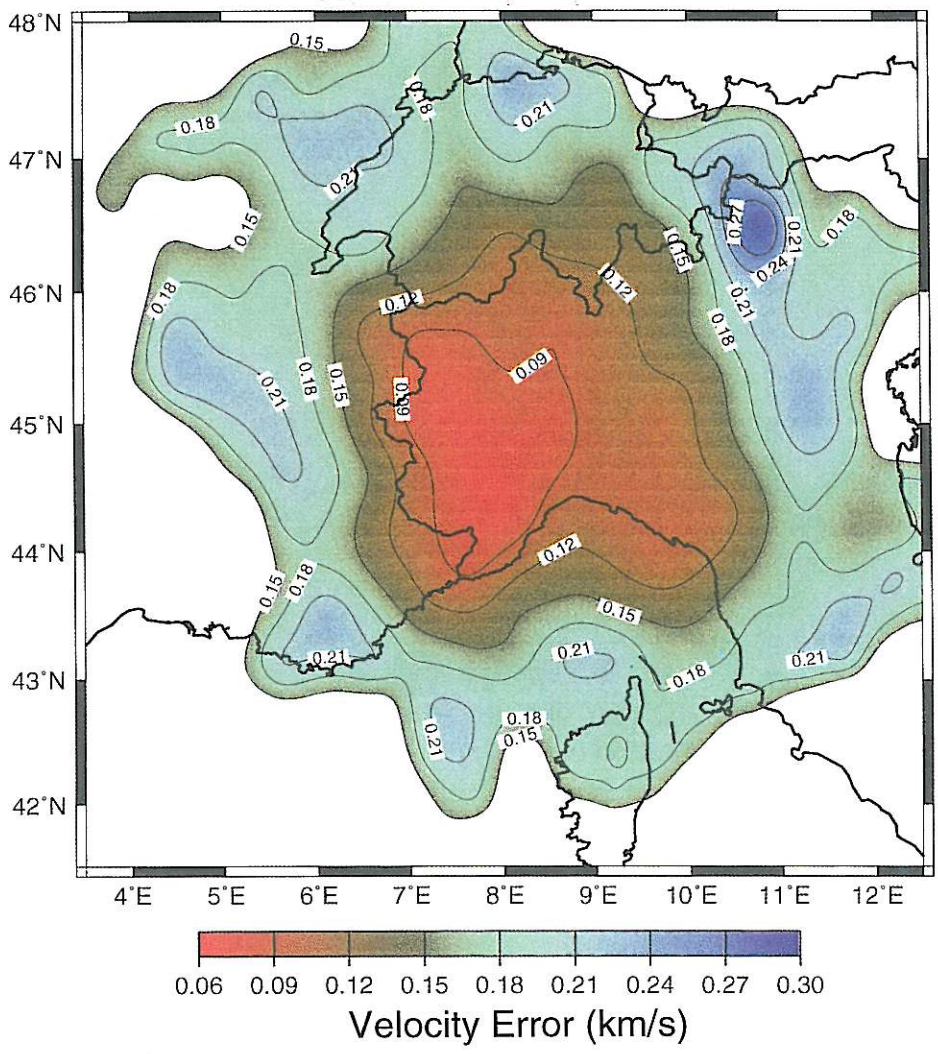

Fig. 8. Standard deviation of the cell velocity as computed by 1000 bootstrap inversion iterations.

Finally, comparing the sensitivity test results for the checkerboard model (fig. 6a) with the velocity error map (fig. 8) it is worth noting that some regions of the sampled area, where the checkerboard pattern appears carefully retrieved (South-Western France, Eastern Po plain), are also affected by large bootstrap errors exceeding 0.2 km/s. In our opinion, this demonstrates that assessing the reliability of the tomographic results only through numerical simulation can be misleading, especially when computing the synthetics from one test model alone.

In conclusion, only the perturbations imaged in the central part of the model showing both velocity error lower than 0.15 km/s and a careful reconstruction of the test models can yield results not prone to misinterpretation.

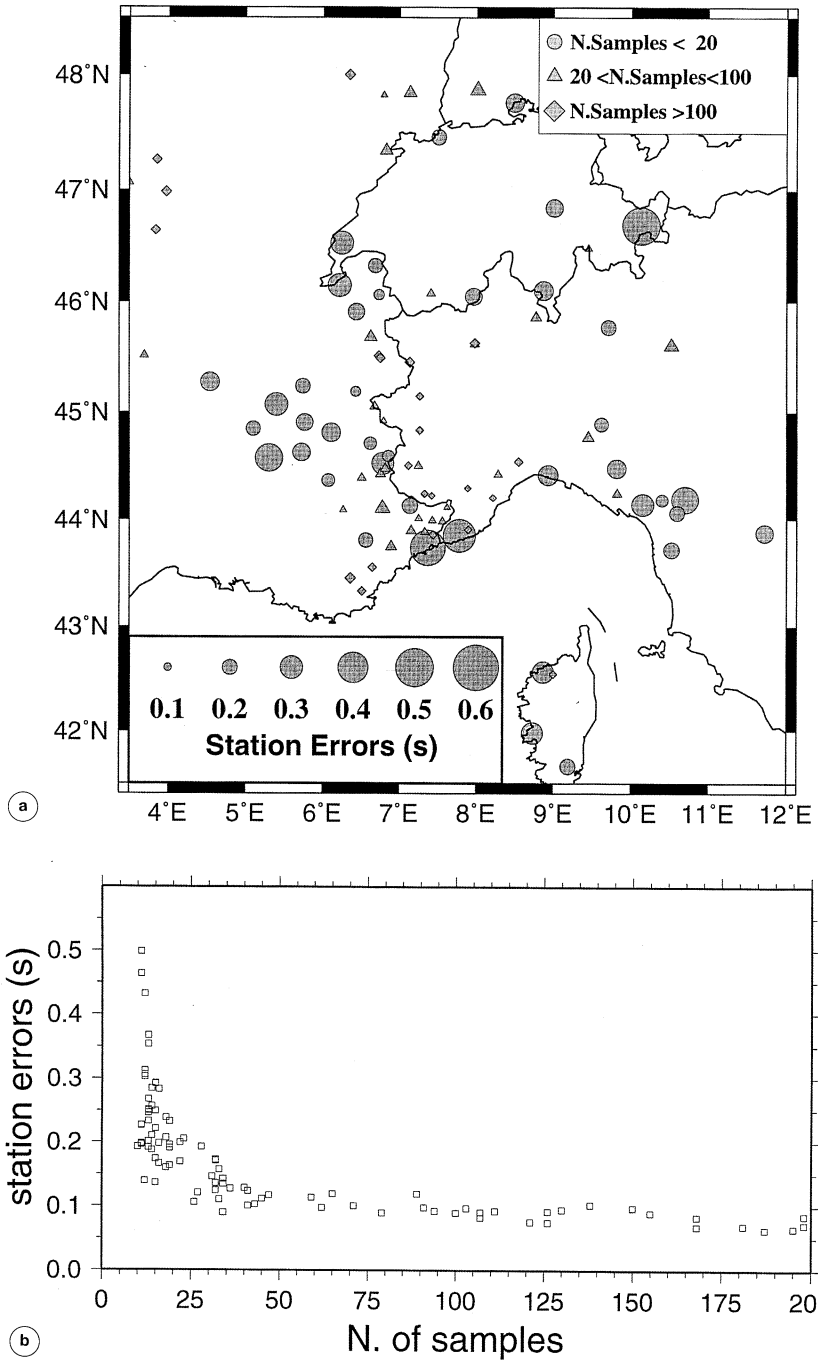

Fig. 9a,b. Standard deviation for station delay times as computed by 1000 bootstrap inversion: a) map of the estimated standard deviations; b) estimated standard deviations *versus* number of samples for each station.

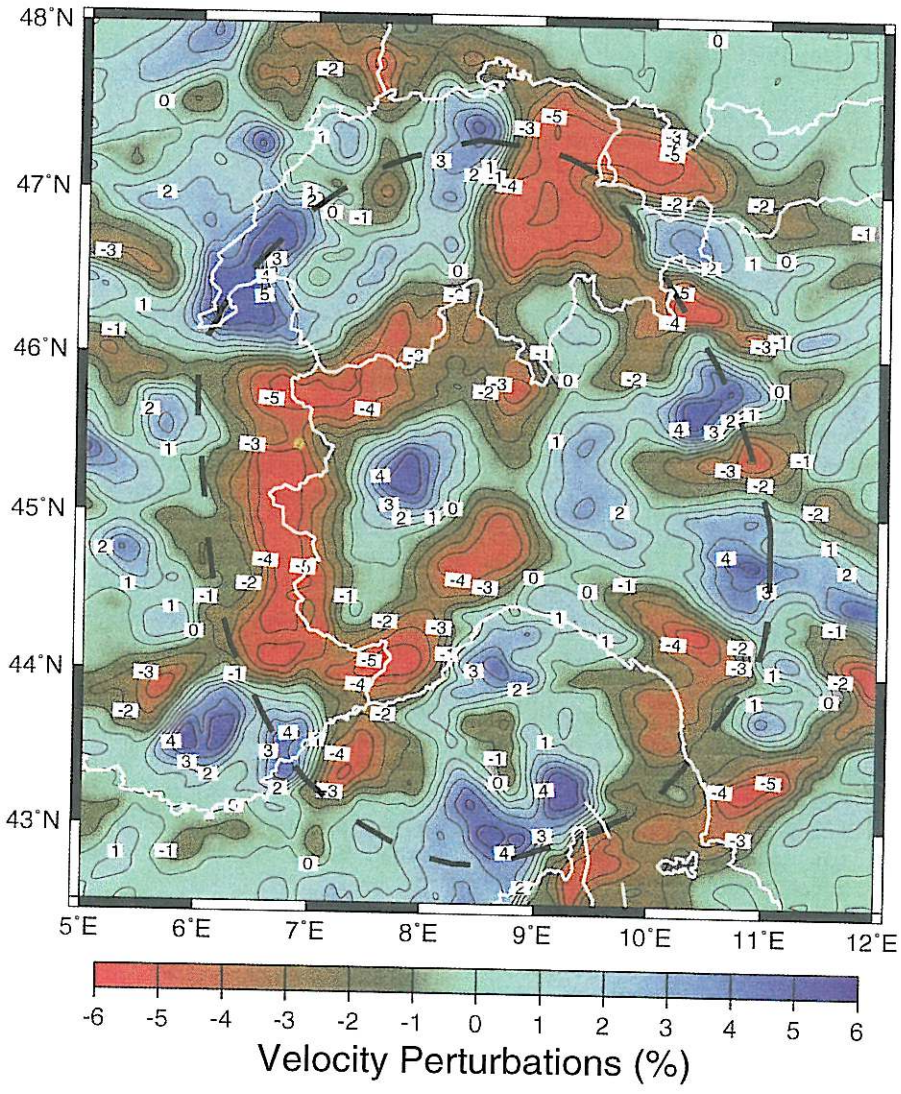

Fig. 10. P_n velocity perturbations in North-Western Italy. Dashed black line circumscribes the area of the tomographic image where the velocity perturbations can be considered reliable.

5. Results

The tomographic image of the lateral P_n wave velocity variation, resulting from this study, was obtained by stopping the inversion procedure after 90 LSQR iterations; assuming a control parameter λ equal to 3 the initial standard error of the observed residuals (0.81 s) dropped to a final value of 0.50 s.

Figure 10 shows the map of the imaged velocity anomalies, expressed as a percentage of the initial velocity, obtained by averaging 25 inversion results of the same cell size, shifted each time by one fifth cell dimension along the

x and y directions (Evans and Zucca, 1988; Cattaneo and Eva, 1990; Evans and Achauer, 1993).

A careful analysis of the reliability test and bootstrap errors has led us to assess the qualitative/quantitative degree of reliability to the model. In particular, figs. 6a and 8 have been considered references to determine the area of the tomographic image in which the results can be considered reliable (black dashed line in fig. 10).

Despite the broadening of the data set the imaged anomalies confirm the results obtained by Parolai *et al.* (1997) even if the blurring of the perturbations in the ray direction is strongly reduced along the edge of the model.

The imaged P_n wave velocity anomalies, ranging from -6% to $+5\%$, can be considered apparent mantle perturbations; they are due to a combination of different effects such as perturbations of the velocity in the upper mantle, crustal thickening and crustal velocity variations.

Looking at fig. 10 it is worth noting the existence of a strong anomalous zone along the Italian-French border showing lateral velocity contrasts reaching 10%.

This region, that in accordance with the reliability tests (see figs. 6, 7 and 8) appears one of the most reliable, shows two consistently low velocity anomalies, underlying respectively the outer side of the Alps and the Monferrato zone, which surround a high velocity perturbation in the inner side of Western Alps that stretches in the N-NE/S-SW direction.

A low velocity area is also present in the North-Western Apennines, from the main divide of the chain to the Ligurian sea. A high P_n velocity centered in the Po plain borders the Northern Apennine limit and appears to extend into the north-east direction to Lake Garda. These anomalies all join together in a horseshoe shape. This area, even if it belongs to a model region with a minor degree of reliability, may be considered sufficiently well resolved taking into account that the errors evaluated with the bootstrap method (0.2 km/s, *i.e.* 2.5% of perturbation) are well below the size of the imaged velocity contrast (8%).

Similar considerations may be extended to Switzerland where the reliability tests give somewhat controversial indications. While the second synthetic model (fig. 7a) indicates good resolution, the checkerboard synthetic (fig. 6a) and bootstrap inversion (fig. 8) show higher reliability only in the Southern Swiss sector.

In the Ligurian sea high velocities are shown close to the coast lines of Liguria and Corsica while mean velocities are found in the middle of the Ligurian basin. Nevertheless, the maxima centered near Corsica can be unrealistic being affected by large errors probably due to the paucity of ray coverage, as shown by the bootstrap results.

The station static delays of fig. 11 span over 2 s. Comparing these results with the maps of synthetic tests and bootstrap analysis, the delays appear suitably resolved only in the central part of the model. As previously stated, the resolution power is strongly related to a full azimuthal ray coverage, but in general for well sampled stations the delays are much larger than the corresponding errors computed with the bootstrap method (fig. 8). In spite of this, as the Moho topography in this area is not smooth and the starting model is too crude, it is not possible to extrapolate a map of the Moho depth out of the station delay times (Hearn and Ni, 1994).

The differences observed between neighbouring stations might be related not only to relative crustal thickness variations and local crustal velocity changes, but also to systematic errors in the original travel time picks. Positive delays follow the outer side of the Alps and the North-Western Apennines where both a strong crustal thickening and the existence of light materials have been found. In contrast, negative delays are found at the margin of the Ligurian sea where the rising of the Moho has been suggested (Giese and Buness, 1992).

In the Western Alps, stations close to the Italian-French border exhibit strong negative delays that are not in agreement with the present knowledge of Moho depth; therefore they might be related to higher crustal velocities.

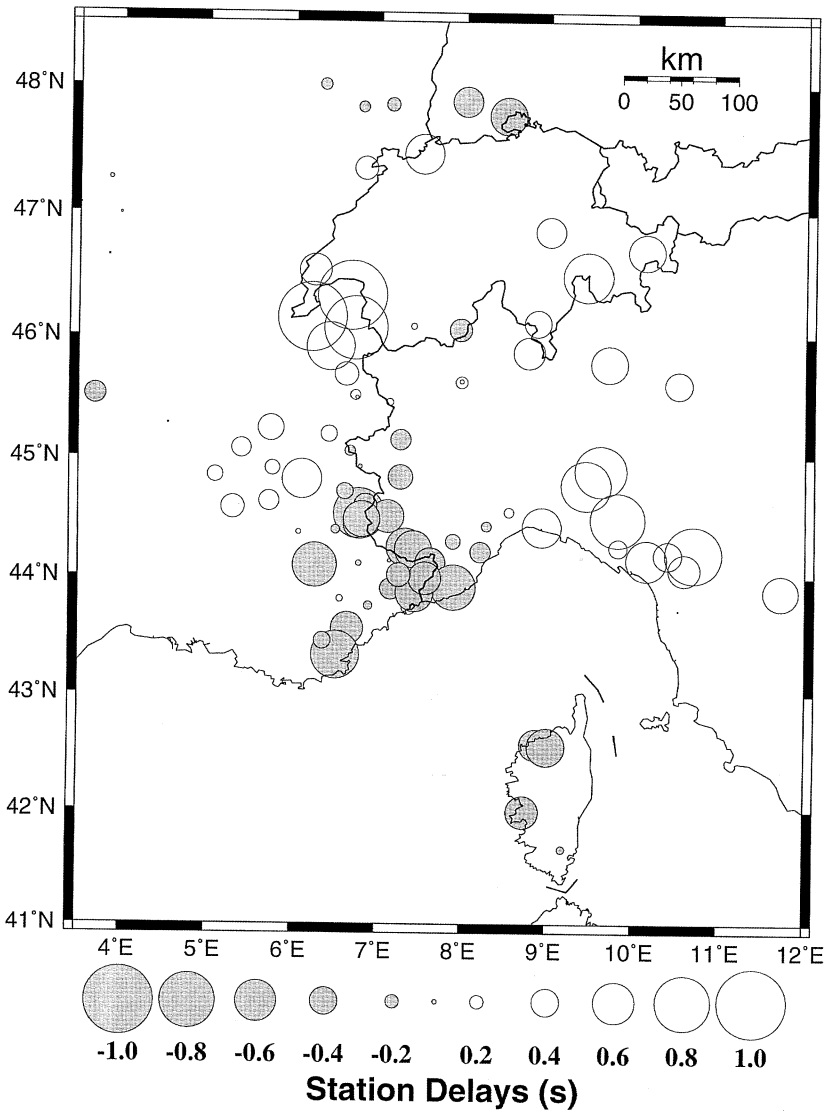

Fig. 11. Crustal station delays: the radius of the circle is proportional to the size of station delays.

6. Discussion and conclusions

The application of synthetic and bootstrap methods has demonstrated that the reliability of the inversion results can be better estimated using different approaches. In some cases the use of numerical simulations alone cannot guarantee that the tomographic images will not be misinterpreted.

Synthetic tests help to qualitatively define the resolution power related to the geometrical parametrization of the model and to the ray

path coverage, while the bootstrap quantification of delay times and velocity errors is sensitive to data errors. Obviously bootstrap standard deviation cannot reflect errors derived by a wrong choice of the mean parameters of the starting model. Moreover, as the time term equation is considered efficient enough to resolve lateral velocity variations in the upper mantle in the presence of a smooth Moho topography, standard deviations of station delays cannot be used to estimate absolute errors in crustal thickness evaluation in such a complicated convergence plate area.

Despite these limitations the application of this method to the high structural complexity of the investigated region has given interesting results that can be interpreted either in terms of crustal thickness lateral variation or as subcrustal velocity perturbations.

As deep crustal roots may act as impedimental structures for the *P*-wave propagation, the low velocity anomalies found in the Alpine region can be related to the crustal thickness, which reaches 55 km beneath the north-western side of the Alps and in Eastern Switzerland (Hitz, 1995). In this case anomalies are also in agreement with the strongest negative Bouguer anomaly (fig. 12) and with a positive slowness perturbation imaged by teleseismic tomography (Solarino *et al.*, 1996).

The high velocity (approximately in direction NNE-SSW) that borders the eastern part of the Western Alps is related to an infracrustal high velocity body (Ivrea body); the wider dis-

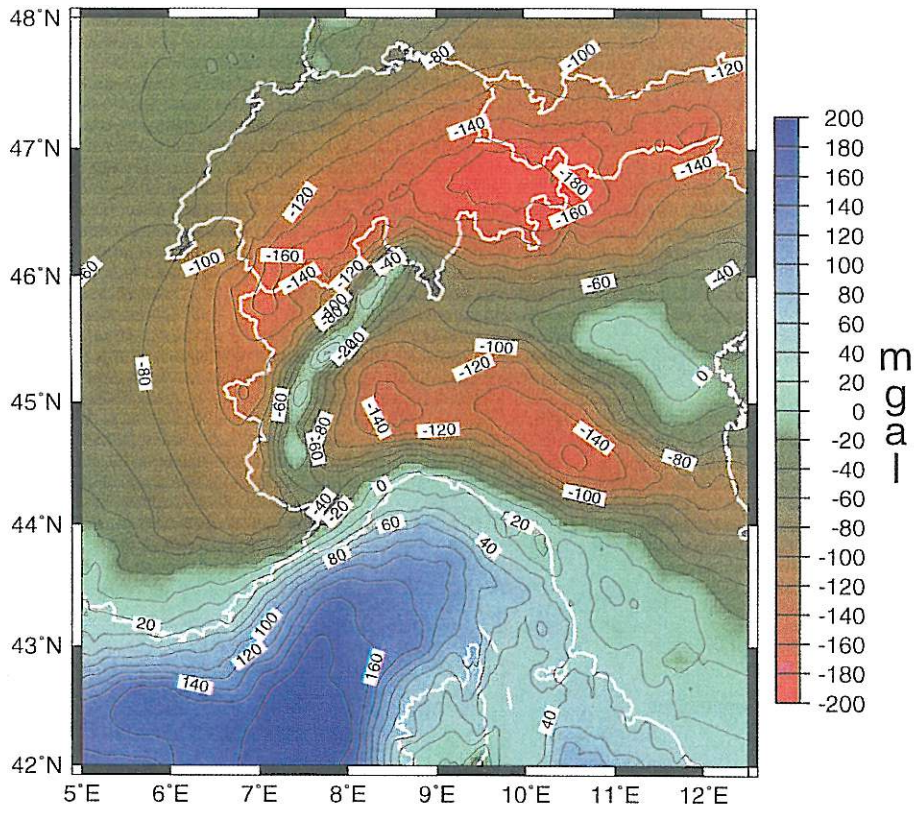

Fig. 12. Contour map of the Bouguer anomalies from EGT data (Klingele *et al.*, 1992).

tribution of this anomaly with respect to the gravimetric one might be ascribed to a defocusing effect of seismic rays due to the Moho surface undulations.

The crustal model proposed by Giese and Buness (1992), more recently revised by Kissling (1993) adopting a quality criteria to screen available geophysical data, entails the deepening of the Adria block beneath a thinned Ligurian crust down to 40-45 km in Western Liguria. This crustal setting could justify the lateral variation of P_n wave velocity imaged in this area. The Ligurian sea shows high velocity, while the negative perturbations imaged beneath the Monferrato zone support the hypothesis of crustal doubling.

On the other hand, the normal P_n velocity (less than 1% perturbation) found between the Ligurian and Corsican coastlines, might be determined by the prevailing effect of an upper mantle velocity of about 7.6-7.7 km/s as revealed by refraction profiles (Egger, 1992) against a dome shaped Moho discontinuity rising up to 15 km depth. The possible existence of crustal indenting of the Ligurian sea mantle hypothesized in the North-Western Apennines (Giese and Buness, 1992; Laubscher *et al.*, 1992) and also emphasized by tomographic studies carried out in the region (Solarino *et al.*, 1996) may correspond to a low velocity zone aligned along the Tyrrhenian side and involving all the Apenninic sectors.

Moreover, the shape and dimension of this anomaly correspond to an anomalous rising of the Moho, characterized by a velocity of 7.4 km/s, depicted in a tectonic sketch map derived from seismic profiles (Boccaletti *et al.*, 1985). Such anomaly borders on the North with the high velocity zone imaged beneath the center of the Po plain. Despite the wider negative Bouguer gravimetric anomaly depicted in the region (fig. 12), this velocity behaviour could be related to the bending of the Padanian Moho deepening both in the Apenninic and Alpine sides.

This geometrical setting of the Moho, also confirmed by the experimental results of the EGT project (Scarascia and Cassinis, 1992), can be related to a geodynamical evolution of the Alpine-Apenninic system consisting of the overthrusting of the Apennines on the Po plain which is, at the same time, forced to underthrust the Southern Alps (Castellarin and Vai, 1986).

In conclusion, as also suggested by the general coherence between the P_n wave anomalies and the Bouguer gravimetric map, it is possible to affirm that, even if the adopted model represents a great simplification of the Earth structure, the obtained results are in agreement with previous geophysical studies meant to determine the Moho topography and the upper mantle velocities. Moreover the P_n wave propagation anomalies imaged reveal the existence of possible crustal doubling beneath the Monferrato zone as also suggested by the analysis of seismic refraction profiles.

Only a complete knowledge of the current structural setting will make it possible to reconstruct the many geodynamical processes that have followed one another in such a small area from the Cretaceous period to the present day.

Acknowledgements

Two anonymous reviewers provided valuable comments that significantly improved the content of the manuscript. We thank P. Augliera, M. Cattaneo and E. Kissling for useful discussion and comments. Map figures used the GMT-System software (Wessel and Smith, 1991).

REFERENCES

ALESSANDRINI, B., L. BERANZOLI and F. MELE (1995): 3D crustal *P*-wave velocity tomography of the Italian region using local and regional seismicity data, *Annali di Geofisica*, **38** (2), 189-211.

BOCCALETTI, M., M. COLI, C. EVA, G. FERRARI, G. GIGLIA, A. LAZZAROTTO, F. MERLANTI, R. NICOLICH, G. PAPANI and P. POSTPISCHL (1985): Consideration on the seismotectonics on the Northern Apennines, *Tectonophysics*, **117**, 7-38.

BRALLE, L.W., W.J. HINZE, R.R.B. VON FRESE and G.R. KELLER (1989): Seismic properties of the crust and uppermost mantle of the conterminous United States and adjacent Canada, in *Geophysical Framework of the United States*, edited by L.C. PAKISER and W.D. MOONEY, *Geol. Soc. Am. Mem.*, **172**, 655-680.

BUNESS, H., P. GIESE, A. HIRN, S. NADIR and S. SCARASCIA (1990): Crustal structure derived from seismic

refraction between Southern Alps and the Ligurian sea, in *Proceedings of the Sixth Workshop on the EGT Project: Data Compilations and Synoptic Interpretation*, edited by R. FREEMAN and S. MUELLER, 165-167.

CASTELLARIN, A. and G.B. VAI (1986): Southalpine versus Po plain Apenninic arcs, in *The Origin of the Arcs*, edited by F.C. WEZEL, 253-280.

CATTANEO, M. and C. EVA (1990): Propagation anomalies in North-Western Italy by inversion of teleseismic residuals, *Terra Nova*, **2**, 577-584.

DEWEY, J.F., M.L. HELMAN, E. TURCO, D.H.W. HUTTON and S.D. KNOTT (1989): Kinematics of the Western Mediterranean, in *Alpine Tectonics, Geological Society of London, Special Publication*, vol. 45, 265-283.

EFRON, B. (1979): Bootstrap methods, another look at the jacknife, *Ann. Stat.*, **7**, 1-26.

EGGER, A. (1992): A lithospheric structure along a transect from the Northern Apennines to Tunisia derived from teleseismic refraction data, *Ph.P. Thesis*, ETH Zürich.

EVANS, J.R. and U. ACHAUER (1993): Teleseismic velocity tomography using the ACH method: theory and application to continental-scale studies, in *Seimic Tomography: Theory and Practice*, edited by H.M. IYER and K. HIRARA (Chapmann and Hall, London), 319-357.

EVANS, J.R. and J.J. ZUCCA (1988): Active high-resolution seismic tomography of compressional wave velocity and attenuation structure at Medicine Lake volcano, Northern California Cascade Range, *J. Geophys. Res.*, **93**, 15016-15036.

GIESE, P. and H. BUNESS (1992): Moho depth, in *A Continent Revealed. The European Geotraverse. Atlas of Compiled Data*, edited by P. BLUNDELL, R. FREEMAN and ST. MUELLER (Cambridge Univ. Press, Cambridge).

GRAND, S.P. (1990): A possible station bias in travel time measurements reported to ISC, *Geophys. Res. Lett.*, **17**, 17-20.

HEARN, T.M. (1984): P_n travel times in Southern California, *J. Geophys. Res.*, **89**, 1843-1855.

HEARN, T.M. and R.W. CLAYTON (1986): Lateral velocity variations in Southern California. II. Results for the lower crust from P_n waves, *Bull. Seism. Soc. Am.*, **76**, 511-520.

HEARN, T.M. and J.F. NI (1994): P_n velocities beneath continental collision zones: the Turkish-Iranian Plateau, *Geophys. J. Int.*, **117**, 273-283.

HEARN, T., N. BEGHOUL and M. BARAZANGI (1991): Tomography of the Western United States from regional arrival times, *J. Geophys. Res.*, **96**, 16369-16381.

HITZ, L. (1995): The 3D crustal structure of the Alps of the Eastern Switzerland and Western Austria interpreted from a network of deep-seismic profiles, *Tectonophysics*, **248**, 71-96.

KISSLING, E. (1993): Deep structure of the Alps – What do we really know?, *Phys. Earth Planet. Int.*, **79**, 87-112.

KLINGELÈ, E., B. LAHMEYER and R. FREEMAN (1992): Bouguer gravity anomalies, in *A Continent Revealed. The European Geotraverse. Atlas of Compiled Data*, edited by P. BLUNDELL, R. FREEMAN and ST. MUELLER (Cambridge Univ. Press, Cambridge), 27-30.

KOCH, M. (1992): Bootstrap inversion for vertical and lateral variations of the *S*-wave structure and the *vp/vs* ratio from shallow earthquakes in the Rhinegraben seismic zone, Germany, *Tectonophysics*, **210**, 91-115.

LAUBSCHER, H., G.C. BIELLA, R. CASSINIS, R. GELATI, A. LOZEJ, S. SCARASCIA and I. TABACCO (1992): The collisional knot in Liguria, *Geologische Rundsch.*, **81/2**, 275-289.

LEES, J.M. and R.S. CROSSON (1989): Tomographic inversion for three-dimensional velocity structure at Mount St. Helens using earthquake data, *J. Geophys. Res.*, **94**, 5716-5728.

LEVEQUE, J.J., L. RIVERA and G. WITTLINGER (1993): On the use of the checker-board test to assess the resolution of tomographic inversions, *Geophys. J. Int.*, **115**, 313-318.

PAIGE, C.H. and M.A. SAUNDERS (1982): Algorithm 583, LSQR: Sparse linear equations and least squares problems, *ACM Transactions on Mathematical Software*, **8**, 195-209.

PAROLAI, S., P. SPALLAROSSA and C. EVA (1997): Lateral variations of P_n wave velocity in North-Western Italy, *J. Geophys. Res.* (in press).

POLINO, R., G. V. DAL PIAZ and G. GOSSO (1990): Tectonic erosion at the Adria margin and accretionary process for the Cretaceous orogeny in the Alps, in *Deep Structure of the Alps*, edited by F. ROURE, P. HEITZMANN and R. POLINO, *Mem. Soc. Geol. Fr.*, Paris, 156, *Mem. Soc. Geol. Suisse*, Zürich, 1, vol. spec. *Soc. Geol. It.*, Roma, **1**, 345-367.

SCARASCIA, S. and R. CASSINIS (1992): Profili sismici a grande angolo esplorati in prossimità del tracciato del profilo CROP 01: una raccolta dei risultati e qualche revisione, *Studi Geologici Camerti*, Volume Speciale (1992/2), CROP 1-1A, 17-26.

SOLARINO, S., P. SPALLAROSSA, S. PAROLAI, M. CATTANEO and C. EVA (1996): Litho-asthenospheric structures of Northern Italy as inferred by teleseismic waves tomography, *Tectonophysics*, **260**, 271-290.

SPAKMAN, W. and G. NOLET (1988): Imaging algorithms, accuracy and resolution in delay time tomography, in *Mathematical Geophysics*, edited N.J. VLAAR, G. NOLET, M.J.R. WORTEL and S.A.P.L. CLOETINGH (D. Reider, Dordrecht), 155-188.

WESSEL, P. and W.H.F. SMITH (1991): Free software helps map and display data, *EOS Trans. Am. Geophys. Un.* **72**, 441.

WILLMORE, P.L. and A.M. BANCROFT (1960): The time term approach to refraction seismology, *Geophys. J. R. Astron. Soc.*, **3**, 419-432.